Magnetic and electronic properties of $NpCo_2$: Evidence for long-range magnetic order

J. P. Sanchez,[1] J.-C. Griveau,[2] P. Javorsky,[2,*] E. Colineau,[2] R. Eloirdi,[2] P. Boulet,[2,†] J. Rebizant,[2] F. Wastin,[2] A. B. Shick,[2,3] and R. Caciuffo[2]

[1]*SPSMS, UMR-E CEA/UJF-Grenoble1, INAC, F-38054 Grenoble cedex, France*

[2]*European Commission, Joint Research Centre, Institute for Transuranium Elements, Postfach 2340, D-76125 Karlsruhe, Germany*

[3]*Institute of Physics, ASCR, Na Slovance 2, CZ-18221 Prague, Czech Republic*

(Received 31 January 2013; published 10 April 2013)

The magnetic and electronic properties of the cubic Laves phase intermetallic compound $NpCo_2$ have been investigated by magnetization, specific heat, and electrical resistivity measurements. Magnetization data confirm previous results, i.e., an antiferromagneticlike order at 12.5 K and a metamagnetic transition at $B_m \sim 4.3$ T at 3 K with a saturation moment of $\sim 0.6\ \mu_B$. Although extensive neutron diffraction studies failed to establish the nature of the antiferromagnetic order, its occurrence is confirmed by specific heat measurements that also highlight the presence of magnetic fluctuations suppressed by the application of an external field larger than B_m. The observed high value of the electronic specific heat, $\gamma_0 \sim 330$ mJ/mol K^2 as $T \to 0$, and the minute magnetic entropy, $<0.1R\ln 2$, classify $NpCo_2$ as an itinerant, moderately-heavy-fermion antiferromagnet. The electrical resistivity data agree with the presence of an antiferromagnetic order below B_m and suggest a non-Fermi liquid behavior at low temperature. The electronic structure of $NpCo_2$ was examined theoretically and compared to experimental data. Local spin density approximation (LSDA) calculations show that this material is close to a magnetic instability and that ferromagnetic alignment of the Np moments is the most stable. LSDA + U calculations in the fully localized limit with $U = 0$ give reasonable agreement with the experimental Np moment value and their orbital and spin contributions.

DOI: 10.1103/PhysRevB.87.134410 PACS number(s): 75.30.Mb, 75.50.Ee, 71.20.Lp

I. INTRODUCTION

The study of the electronic and magnetic properties of the intermetallic NpX_2 cubic Laves phases (C-15 type face-centered cubic structure, with Np atoms at 000 and $\frac{1}{4}\ \frac{1}{4}\ \frac{1}{4}$ positions, and X atoms arranged in tetrahedra around $\frac{3}{4}\ \frac{3}{4}\ \frac{3}{4}$ and symmetry related points) has attracted considerable attention during the last four decades,[1–6] owing to the fact that their actinide spacings d_{Np} are close to the Hill limit ($\sim$3.2 Å),[7] below which the magnetic order cannot be sustained. The short interatomic distances and the high degree of delocalization of the $5f$ electrons in these systems favor a direct $5f$-$3d$ hybridization, with important effects on the magnetic properties. The "Hill" ansatz is well obeyed when the X partner is nonmagnetic, e.g., $NpRu_2$ which lies just below the Hill limit does not order magnetically, whereas $NpOs_2$ and $NpIr_2$, situated just above it, present ferromagnetic and antiferromagnetic order, respectively.[8] The situation is more complicated if the X partner is a magnetic $3d$ metal, as Mn, Fe, Co, or Ni. In those cases, NpX_2 orders magnetically, even though $d_{Np} < 3.2$ Å.[1,2] $NpCo_2$, the subject of the present investigation, is particularly interesting as the nature of its magnetic ground state is still under debate.[6] On the basis of magnetization and ^{237}Np Mössbauer data, $NpCo_2$ is generally listed as a weakly anisotropic antiferromagnet ($T_N \sim 13$ K) exhibiting a low-temperature metamagnetic transition at moderate external field values. Mössbauer spectroscopy reveals an unusual behavior, with the coexistence of static ($\sim 0.5\ \mu_B$) and fluctuating magnetic moments even at temperatures approaching 0 K.[6] Despite numerous attempts, neutron diffraction studies on both polycrystalline and single-crystal $NpCo_2$ samples failed to observe superlattice Bragg reflections associated to long-range antiferromagnetic order.[2,6] Short-range order or spin-glass freezing was then suggested, although the latter appears to be ruled out by magnetization measurements.[6] The strongest argument in favor of long-range order stabilization was provided by muon spectroscopy[9] that clearly shows the onset of a spontaneous spin precession below 12.5 K. The temperature dependence of the precession frequency strictly follows the magnetization curve, whereas the strong damping of the signal points towards a complex spin structure.

Here we report the results of low-temperature specific heat measurements, performed in external magnetic fields up to 9 T, in order to gain further information on the properties of $NpCo_2$. The observation of a well defined peak at T_N is a clear signature of transition to long-range antiferromagnetically ordered phase. Specific heat data of the nonmagnetic isostructural UCo_2 compound are also presented with the initial aim to estimate the phonon contribution to the specific heat of $NpCo_2$. In addition we present magnetization curves and electrical resistivity data. The results of first-principle electronic structure calculations are also presented and compared to experimental data.

II. EXPERIMENTAL DETAILS

The $NpCo_2$ single crystals used in this study were grown by using the Czochralski technique at the Institute for Transuranium Elements of the Joint Research Centre, Karlsruhe.[3] They came from the same batch used for the neutron diffraction experiments.[3,6] Since the magnetic properties of $NpCo_2$ are known to be very sensitive to the stoichiometry,[1,10] the single crystals were carefully characterized with unpolarized neutron diffraction using a four-circle neutron diffractometer. The samples are within 1% of stoichiometry[3] with a lattice parameter $a = 7.028$ Å at 4.2 K.[11] A polycrystalline sample of the isostructural compound UCo_2 ($a = 6.997$ Å) was

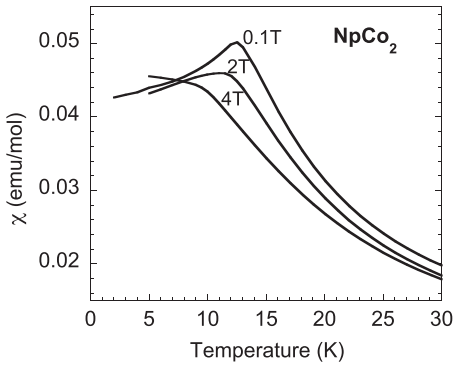

FIG. 1. Temperature dependence of the magnetic susceptibility of the $NpCo_2$ single crystal for different magnetic field oriented along the [100] easy axis.

prepared by arc melting stoichiometric amounts of uranium and cobalt metals under argon atmosphere. The phase purity of the sample was checked by x-ray powder diffraction that showed no secondary phases.

Direct current magnetization measurements of $NpCo_2$ were carried out on a Quantum Design SQUID magnetometer (MPMS-7) in magnetic fields up to 7 T on a 29-mg single crystal. The specific heat experiments were performed by the relaxation method using the same $NpCo_2$ single crystal and a 23-mg polycrystalline UCo_2 sample in a Quantum Design PPMS-9 within the temperature range 2–300 K and magnetic field up to 9 T. The electrical resistivity of $NpCo_2$ was measured on the PPMS-9 system by a dc-four-probe technique on a 0.8-mm^3 single crystal and in fields up to 9 T.

III. EXPERIMENTAL RESULTS

A. Magnetization of $NpCo_2$

As shown before on a powdered sample,[6] the susceptibility $\chi(T)$ at low fields ($B \leqslant 3$ T) presents a maximum (e.g., $T_N \sim 12.5$ K at 0.1 T) which is slightly shifted to lower temperatures with increasing applied fields, whereas a progressive leveling-off of $\chi(T)$ is observed below T_N. With an applied field of 4 T no maximum is observed; instead $\chi(T)$ increases continuously with decreasing temperature (Fig. 1).

Isothermal magnetization curves recorded between 3 and 20 K in fields up to 7 T applied along the easy [100] axis are displayed in Fig. 2. The curve measured with the sample kept at 3 K clearly signals the occurrence of a metamagnetic transition at a field of about $B_m \sim 4.3$ T, estimated by computing the derivative of the magnetization with respect to the field dM/dB (inset in Fig. 2). No hysteresis is observed at the transition. Above B_m the magnetization reaches $\sim$0.55 μ_B/f.u. at our maximum field of 7 T, a value slightly below the saturation value ($\sim$0.60 μ_B/f.u.) estimated previously.[6]

B. Specific heat measurements

1. *Specific heat of UCo_2*

The specific heat data for UCo_2 are presented in Fig. 3. The inset shows a plot of C/T vs T^2 for $T < 14$ K. The application

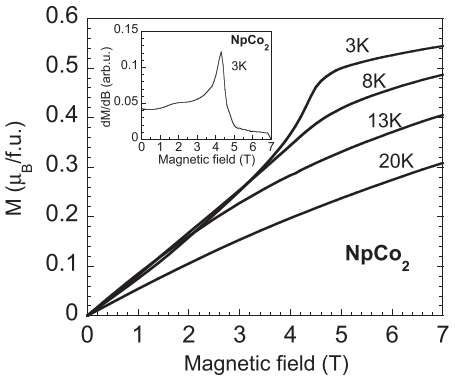

FIG. 2. Isothermal magnetization curves of the $NpCo_2$ single crystal for the magnetic field applied along the [100] easy axis. The inset shows the field dependence of dM/dB at 3 K used to estimate the metamagnetic transition field.

of a 9 T external field does not produce significative changes. A "high" temperature (T > 8 K) analysis of the measured data gives $\gamma < 5$ mJ/K^2 mol and $\beta = 1$ mJ/K^4 mol in the expression $C/T = \gamma + \beta T^2$. Similar results were found by Franse *et al.*[12] who pointed out that these values must be considered with caution because they depend on the temperature range used for the analysis.

The specific heat data are further analyzed ($T < 13$ K) using the expression[13]

$$C/T = A + BT^2 + D\,T^2 \ln T, \qquad (1)$$

where the last term represents the contribution responsible for the deviation from a simple metallic behavior. The parameters A, B, and D obtained by fitting the experimental data to Eq. (1) are reported in Table I, together with the values previously obtained by Frings and Franse.[14]

The specific heat of UCo_2 exhibits the temperature dependence expected for a spin fluctuation system and may be compared with the theory which predicts[13]

$$\frac{C}{T} = \gamma\frac{m^*}{m} + \beta T^2 + \left(\frac{\alpha\gamma}{T_{SF}^2}\right) T^2 \ln\left(\frac{T}{T_{SF}}\right), \qquad (2)$$

where m^* and m are the enhanced and bare values of the electron mass; γ is the electronic specific heat coefficient; α is

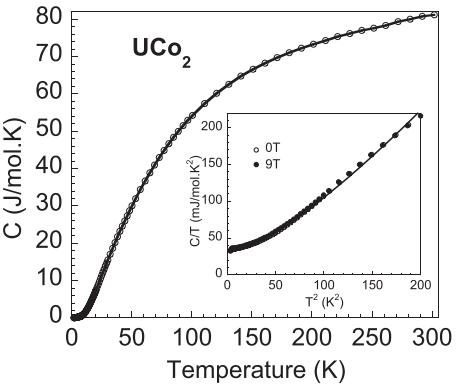

FIG. 3. Specific heat of UCo_2 at zero field. The inset shows a plot of C/T vs T^2 at 0 T (○) and at 9 T (●); the solid line in the inset represents a fit to expression (1).

TABLE I. Specific heat of UCo_2; best-fit values of the parameters appearing in the expression $C/T = A + BT^2 + DT^2 \ln T$, with C in mJ/K mol and T in K.

Temperature range (K)	A	B	D	Reference
1.3–8.7	36.8 (4)	−0.9 (1)	0.69 (4)	Ref. 14
1.5–13	36.2 (9)	−1.0 (2)	0.72 (5)	This work

a parameter depending on the Coulomb interaction, the density of states at the Fermi level, and the Stoner enhancement factor; βT^2 is the lattice contribution, and T_{SF} the spin fluctuation temperature.

Comparison of expressions (1) and (2) gives $A = \gamma(m^*/m)$, $B = \beta - (\frac{\alpha\gamma}{T_{SF}^2}) \ln T_{SF}$ and $D = \frac{\alpha\gamma}{T_{SF}^2}$. The coefficient β in the expression of B is related to the Debye temperature θ_D via the relation $\beta = \frac{3(1944\times10^3)}{\theta_D^3}$. Using the value of $\theta_D = 238$ K determined for the isostructural compound $LuCo_2$,[15] we estimated $\theta_D^{UCo_2} = 215$ K using the relation $\theta_D^{UCo_2} = \sqrt{\frac{m_{LuCo_2}}{m_{UCo_2}}}\theta_D^{LuCo_2}$ where the m's are the formula masses of the respective compounds. It follows that $\beta = 0.579$ mJ/mol K^4.

Combining the coefficients B and D yields $T_{SF} \sim 8.6$ K. It is lower than those, between 25 and 40 K, reported by Franse *et al.*[12] Note, however, that this value depends strongly on the value chosen for θ_D because β is small. We note that the Debye temperatures given above were deduced to describe the whole phonon spectrum in $LuCo_2$ or UCo_2. In a more realistic approach, the Debye temperature is used to describe the acoustic phonons only. The same $\beta = 0.579$ mJ/mol K^4 would then correspond to the Debye temperature of 150 K. The minute effect of the applied field B on the specific heat of UCo_2 can be accounted for by the theory developed by Béal-Monod *et al.*[16] The shift $\Delta(C/T)$ caused by an applied field is given by the expression $\frac{\Delta(C/T)}{C/T} \approx (\frac{\mu_B B}{k_B T_{SF}})^2 \frac{S}{\ln S}$. With a value for the Stoner exchange enhancement factor S of approximately 3 (Ref. 12), a value for B of 9 T and a value for T_{SF} of 25 K we calculate a relative change in C/T of the order of 1.6% in agreement with the experimental data of Fig. 3 where $\Delta(C/T)$ at 2 K is about 2%. The suppression of the spin fluctuations clearly requires the application of a much higher field which is tentatively estimated to be about 20 T from the deviation from linearity of the magnetic isotherm of UCo_2 at 4.2 K.[12]

2. *Specific heat of $NpCo_2$*

The temperature dependence of the specific heat (displayed as C/T) for $NpCo_2$ in zero field and in various applied magnetic fields up to 9 T is shown in Fig. 4. The most prominent feature is the peak connected with the antiferromagnetic ordering. The shape of this anomaly is typical for a second-order phase transition. The idealization of the specific heat jump at T_N under the constraint of entropy conservation yields an ordering temperature $T_N = (12.8 \pm 0.3)$ K in zero field, well in agreement with the magnetization data. When applying the external field, the peak is progressively shifted to lower temperatures. This behavior is expected for an antiferromagnet. The anomaly disappears in fields above 4.5 T, i.e., above the metamagnetic transition observed in the magnetization data (see Sec. III A). Simultaneously, in fields above the metamagnetic transition, we observe the shift of the magnetic entropy to higher temperatures (see the 6 and 9 T curves in Fig. 4). This is indicative for a polarized ferromagnetic state.

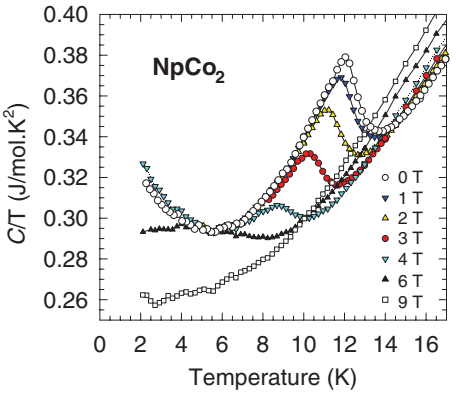

FIG. 4. (Color online) Specific heat of $NpCo_2$ measured in different magnetic fields applied along the [100] crystallographic direction.

Another feature seen in Fig. 4 is the strong upturn at low temperatures. The field development of this upturn is well illustrated in Fig. 5 where we report the field dependence of C/T at 2.5 K. C/T remains about constant (313–322 mJ/mol K^2) up to 4.5 T and then is gradually suppressed with increasing field for $B > 4.5$ T (i.e., in the polarized ferromagnetic state), decreasing to ~260 mJ/mol K^2 at 9 T. One can consider several explanations. For example, such upturn is observed in many neptunium intermetallics as a consequence of the nuclear hyperfine Schottky term due to the splitting of the ^{237}Np nuclear ground state by the hyperfine field.[17,18] For $NpCo_2$ with $B_{hf} = 91.6$ T at 4.2 K,[6] C_{nucl}/T amounts to about 0.4 mJ/mol K^2, i.e., a value too low to explain the observed low-temperature excess of the specific heat. Furthermore, the external field suppresses the upturn which is not consistent with such explanation and we can rule it out. Another possibility is the existence of a second magnetic phase transition at temperatures below 2 K. Although we cannot unambiguously rule it out, the overall behavior in applied fields does not support this hypothesis.

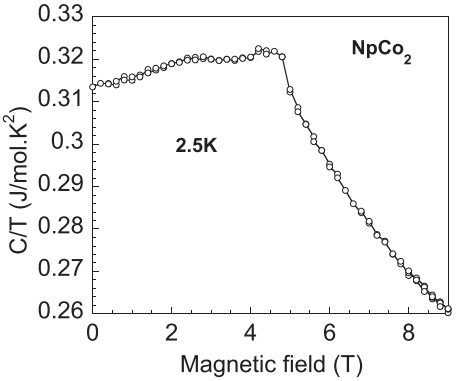

FIG. 5. Magnetic field dependence of the specific heat of $NpCo_2$ at 2.5 K as a function of the magnetic field applied along [100] easy axis.

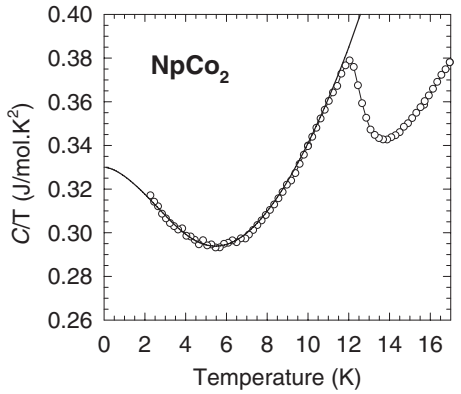

FIG. 6. Low-temperature part of the specific heat of $NpCo_2$ (symbols) and the fit (full line) to formula (3) using the parameters given in the text.

We therefore suggest attributing the observed upturn to spin fluctuations that persist only in the antiferromagnetic state of $NpCo_2$. Such behavior is not unusual and is observed, e.g., in several uranium intermetallics.[19–21] Following the procedure applied also, e.g., for U_2Pd_2In,[19] we use the formula (2) with an additional term $C_{\text{magnon}} = aT^{1/2}\exp(-\Delta/T)$ describing the magnetic excitations across an anisotropic gap Δ in the magnon spectrum. We have thus fitted our zero-field $NpCo_2$ data below T_N to the formula

$$C = \gamma T + \beta T^3 + \delta T^3 \ln(T/T_{SF}) + aT^{1/2}\exp(-\Delta/T). \tag{3}$$

To simplify the fit and to reduce the number of parameters, we assume the same phonon energies as in UCo_2, i.e., $\beta = 0.579\ \text{mJ/mol K}^4$. The best agreement with experimental data is then obtained for $\gamma = 330\ \text{mJ/mol K}^2$, $\delta = 0.0015\ \text{J/mol K}^4$, $T_{\text{SF}} = 23$ K, $a = 3.8\ \text{J/mol K}^{3/2}$, and $\Delta = 27$ K. The specific heat calculated using these values is drawn in Fig. 6. The values should be taken with care as they are correlated to a certain extent and the electronic contribution (γ value) might be temperature dependent. Nevertheless, the large γ value at low temperatures is unambiguous and indicates an extremely large density of states at the Fermi level as observed in other Np-based Laves phases.[22,23] Figure 7 shows the C/T vs T data for $NpCo_2$ and UCo_2 in a broader temperature region up to 100 K. Assuming that the spin-fluctuation and magnetic contributions are negligible well above T_N, the specific heat of both UCo_2 and $NpCo_2$ is a simple sum of the phonon and electronic contributions. Such assumption is confirmed by the fact that the $NpCo_2$ data measured in 0 T and 9 T overlap within the experimental error. The temperature dependence of C/T for UCo_2 agrees well with that of $NpCo_2$ considering only a difference of 33 mJ/mol K^2 for the γ value of the two compounds (see full line in Fig. 7). This confirms that the phonon spectra in UCo_2 and $NpCo_2$ are very similar, as expected. Considering $\gamma_{UCo_2} = 36\ \text{mJ/mol K}^2$, as determined above, we get $\gamma_{NpCo_2} = 69\ \text{mJ/mol K}^2$ for the paramagnetic phase of $NpCo_2$, which is considerably lower than the low-temperature limit but still remarkably high. Below 30 K, when approaching T_N, the specific heat of $NpCo_2$ starts to increase over the paramagnetic dependence due to magnetic fluctuations and/or increasing electronic contribution.

Let us finally estimate the magnetic entropy. Its value can be evaluated by integrating the anomaly around T_N. We obtain roughly the value of $S_{\text{mag}} = 250\ \text{mJ/mol K},^2$ i.e., $\sim 0.05R\ln 2$. Another estimate can be done when integrating the difference between the C/T vs T data measured in 0 and 9 T above T_N (see Fig. 7), which is presumably of magnetic origin. In this way, we get $S_{\text{mag}} \cong 0.1R\ln 2$ comparable to the value found, e.g., for $NpOs_2$ ($\sim 0.2R\ln 2$).[22] The magnetic entropy is rather low which might eventually point to a delocalized nature of the $5f$ electrons in $NpCo_2$ as already anticipated from the reduced ratio of the orbital and spin moment as compared to the free ion expectations.[3,4]

C. Resistivity of $NpCo_2$

The resistivity of $NpCo_2$ above 100 K is nearly temperature independent up to room temperature, where $\rho(300\ \text{K}) \sim 125\ \mu\Omega\,\text{cm}$. Below 16 K a shallow minimum is followed by a flat maximum at about 13 K which corresponds to the T_N value inferred from the magnetization and specific heat data. At lower temperature ρ decreases with decreasing temperatures to a value of $\rho(2\ \text{K}) \sim 85\ \mu\Omega\,\text{cm}$ which gives the ratio $\rho(2\ \text{K})/\rho(300\ \text{K})$ of 0.68 (Fig. 8). The relatively large value of the low-temperature resistivity is often taken as due to a poor

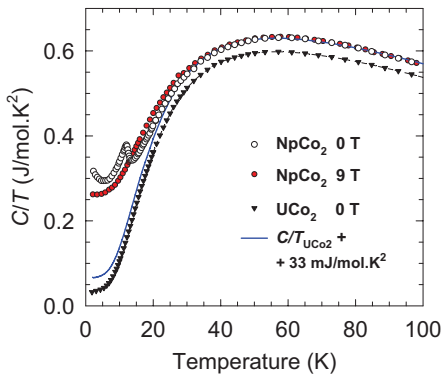

FIG. 7. (Color online) Specific heat of $NpCo_2$ measured in 0 and 9 T together with specific heat of UCo_2 in 0 T. The full (blue) line represents the C/T data of UCo_2 shifted by 33 mJ/mol K^2 to fit the $NpCo_2$ data in the paramagnetic region above $\sim$30 K.

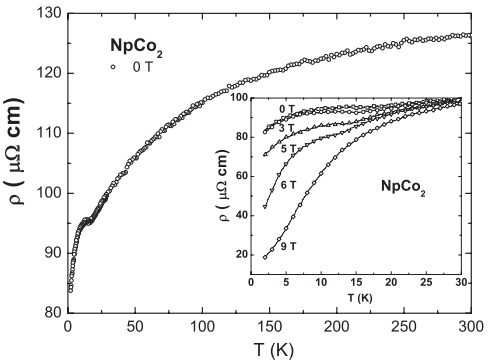

FIG. 8. Zero-field temperature dependence of the resistivity of $NpCo_2$. The current I is parallel to the [100] direction. The inset shows the T dependence of the resistivity at different magnetic fields applied along the [100] easy axis.

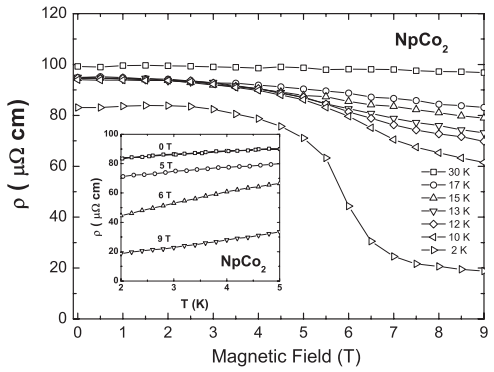

FIG. 9. Magnetic field dependence of the resistivity of $NpCo_2$. The inset shows the linear low-temperature dependence of the resistivity at selected magnetic fields.

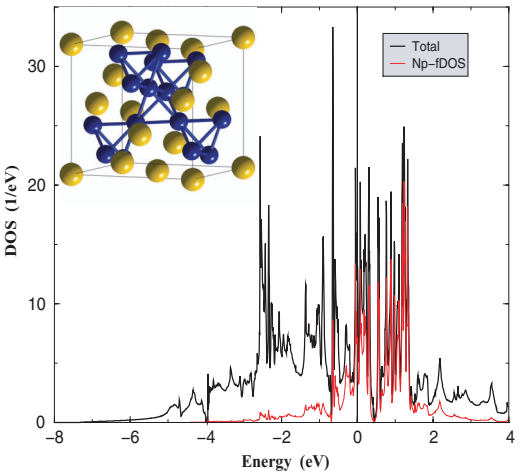

FIG. 10. (Color online) Total and Np-atom projected DOS for $NpCo_2$. The inset shows the cubic Laves C15 structure of $NpCo_2$ where the large spheres represent the Np atoms and the small spheres the Co atoms.

quality of the sample. However, as we shall see below (applied field measurements), a large fraction of $\rho(2\ \mathrm{K})$ is related to the antiferromagnetic state of the sample.

Application of an external magnetic field is shown to affect drastically the shape of the resistivity curves (inset of Fig. 8). The shallow minimum and T_N are shifted to lower temperatures and the low-temperature decrease of ρ becomes faster with increasing field. The latter behavior is nicely illustrated in the plot of $\rho(2\ \mathrm{K})$ as a function of the applied field (Fig. 9); $\rho(2\ \mathrm{K})$ remains almost constant up to the metamagnetic transition (∼4.5 T) and then decreases rapidly and displays a weakly saturating tendency analogous to the $M(B)$ behavior (Fig. 2). A value of about 20 $\mu\Omega$ cm is recorded in the high-field limit. The large resistivity changes connected with the metamagnetic transitions in antiferromagnets are usually attributed to the suppression of antiferromagnetic (AF) fluctuations and the disappearance of magnetic superzones when AF ordering is suppressed by a magnetic field.

We found a linear T dependence for $\rho(T, B)$ at temperatures below 4.5 K that points to a possible occurrence of a non-Fermi liquid behavior. Writing $\rho(T,\ B) = \rho_0(B) + a(B)T$ we observed that $\rho_0(B)$ decreases from ∼83 $\mu\Omega$ cm at zero field down to ∼9 $\mu\Omega$ cm at 9 T while $a(B)$ increases from 2.67 $\mu\Omega\,\mathrm{cm\,K^{-1}}$ at zero field up to 5 $\mu\Omega\,\mathrm{cm\,K^{-1}}$ at 9 T with a maximum value of ∼8.33 $\mu\Omega\,\mathrm{cm\,K^{-1}}$ at 6 T.

IV. ELECTRONIC STRUCTURE CALCULATIONS

To examine theoretically the electronic structure of $NpCo_2$ and to make a comparison with experimental data we used in-house implementation[24] of the highly accurate full-potential-linearized augmented plane wave (FP-LAPW) method. This FP-LAPW version includes all relativistic effects: scalar relativistic terms and spin-orbit coupling implemented in a self-consistent second-variational manner. The radii of the atomic "muffin-tin" spheres are set to 2.8 a.u. (Np) and 2.3 a.u. (Co). The parameter $RK_{\max} = 9.8$ determined the basis set size, and the Brillouin zone (BZ) sampling was performed with 729 k points.

A. Density functional theory (DFT) calculations

First we used the local density approximation (LDA), and performed the non-spin-polarized relativistic calculations. The corresponding density of states total (DOS) and Np-atom f-projected (f-DOS) are shown in Fig. 10. The high value of DOS at Fermi level, $N(E_F)$ (per unit cell), of 28.25 $\mathrm{eV^{-1}}$ corresponds to the electronic specific heat coefficient $\gamma = 33.29\ \mathrm{mJ\,K^{-2}\,mol^{-1}}$. This value of γ is of the same order of magnitude as the value of 69 $\mathrm{mJ\,K^{-2}\,mol^{-1}}$ deduced from the specific heat data in the paramagnetic state of $NpCo_2$ (see Sec. III B 2). The computed f occupation $n_f = 3.79$ agrees well with the f occupation obtained in previous band structure calculations (∼3.8) in Ref. 4 and points out again the difficulty to evaluate the f count from Mössbauer isomer shift values in metallic systems.[6]

The Stoner exchange I of 62 meV is evaluated from scalar-relativistic spin-polarized LSDA calculations. The Stoner product $I\,N(E_F)/2 = 0.89$ shows that the material is close to magnetic instability. The Stoner criterion for ferromagnetism (FM) does not apply to $NpCo_2$ in agreement with the experimental findings.

We can estimate the possibility for other than FM types of magnetic instability. The paramagnetic susceptibility $\chi_0\,(q, \omega)$ in the limit of small q and ω can be expanded[25] as

$$\chi_0(q,\omega) = N(E_F) - aq^2 + ib\omega/q.$$

The a coefficient is proportional to the second derivative of the square of the Drude plasma energy $\Omega_p(E)$ over the energy at Fermi level E_F, and the sign of this derivation indicates the type of magnetic instability. A positive sign corresponds to $q = 0$ FM fluctuations, whereas a negative sign corresponds to $q \neq 0$ AF fluctuations. From the cubic polynomial fit to $\Omega_p(E)$, the second derivative of -1108.2 at $E = E_F$ was calculated, suggesting $NpCo_2$ to be susceptible to (AF) instability (including possibly a spin spiral).

Next we performed the LSDA calculations assuming FM and AF initial arrangement of the two Np atoms in the $NpCo_2$ unit cell. What we found is that the spin polarization decreases the total energy with respect to the nonmagnetic solution by 0.121 eV per formula unit (f.u.) for the FM solution and by 0.048 eV/f.u. for the AF solution. The positive (AF–FM) total energy difference of 0.043 eV suggests the FM-ordered

TABLE II. Spin (μ_S), orbital (μ_L), and total ($\mu_J = \mu_{S+}\mu_L$) magnetic moments (μ_B) for the Np and Co atoms in FM and AF $NpCo_2$.

	FM		AF	
	Np	Co	Np	Co
μ_S	2.68	−0.47	1.95	0.00
μ_L	−1.95	−0.01	−1.90	0.00
μ_J	0.73	−0.48	0.05	0.00

ground state. The calculations did not include more complex AF configurations anticipated from the experimental results.

The spin (μ_S), orbital (μ_L), and total ($\mu_J = \mu_{S+}\mu_L$) magnetic moments for the calculations with FM and AF magnetic moments are shown in Table II. It is interesting to note that the moments on Co atoms disappear in the AF case.

B. LDA + U calculations

Next we consider the FM case only and apply to it the LSDA + U, making use of the rotationally invariant relativistic version of LSDA + U, implemented in the FP-LAPW basis.[25,26] We make a comparison with previous LSDA + *orbital polarization* (OP) and experimental results of Wulff *et al.*[3] For the neptunium f shell, the Coulomb U (Slater integral F_0) was varied as a parameter in a range from 0 to 3 eV. Other Slater integrals $F_2 = 7.43$ eV, $F_4 = 4.83$ eV, and $F_6 = 3.53$ eV were selected in accord with commonly accepted values for the exchange $J = 0.61$ eV.[27] Two flavors for LSDA + U double-counting correction were used in the calculations: fully localized limit (FLL) and around mean field (AMF).

The moment values are very sensitive to the choice of the Coulomb U parameters and the choice of LSDA + U double counting (DC). When AMF-DC is used, the magnitude of spin moment stays close to its LSDA value (see Table II) and the orbital moment gets enlarged by 50% for Coulomb $U = 0$. The C_2 ratio has a correct positive sign, but its magnitude is about three times bigger than the experimental value. With an increase of Coulomb U, the absolute value of spin moment is decreasing while the orbital moment is increasing, and the C_2 ratio is decreasing.

For FLL-DC and Coulomb $U = 0$ eV, our calculated spin, orbital, and total magnetic moments, as well as C_2 ratio are close to the scaled experimental (Expt.*; see Table III) data of Ref. 3. The scaling of the individual μ_S and μ_L was introduced in Ref. 3 to reconcile the polarized neutron scattering results in a magnetic field of 4.6 T (Expt. as shown in Table III) with the total Np moment deduced from zero-magnetic-field Mössbauer experimental results, as well as the saturation magnetization measurements in a field of up to 10 T (see discussion in Ref. 3). From the observation that the FM solution for Coulomb $U = 0$ with FLL double counting is in agreement with the scaled experimental data in an external magnetic field, we suggest that as soon as the external magnetic field is strong enough to suppress the dynamical spin fluctuations, the static mean-field LSDA + U theory starts working for $NpCo_2$. The Coulomb $U = 0$ value used in the calculations indicates that Coulomb correlations, beyond those already accounted for in the LSDA part, are fully screened. This is fully consistent with itinerant nature of the f states in $NpCo_2$.

V. CONCLUSION

Single crystals of the binary $NpCo_2$ compound crystallizing in the cubic C-15 type Laves phase structure were examined by magnetization, specific heat, and resistivity measurements. Susceptibility data indicate that $NpCo_2$ orders magnetically at $T_N \sim 12.5$ K while magnetization curves show that a metamagnetic transition sets in at about 4.3 T at 3 K, with a saturation moment of ∼0.6 μ_B. The occurrence of a "long-range" antiferromagnetic order at T_N is confirmed by the specific heat measurements. This is expected to stimulate further neutron diffraction experiments aimed at establishing the nature of the antiferromagnetic order which is anticipated to be complex and probably noncollinear as a consequence of geometric frustration (the Co ions form a lattice of a corner sharing tetrahedra). T_N is shown to be reduced upon applying a magnetic field. The significant low-temperature upturn of the specific heat is attributed to magnetic fluctuations which are suppressed in the polarized ferromagnetic state, i.e., above the metamagnetic transition. The electronic specific heat coefficients of the paramagnetic and ordered states are $\gamma_p \sim 69$ mJ/mol K^2 and $\gamma_0 \sim 330$ mJ/mol K^2, respectively, and the Debye temperature is estimated to amount to 238 K. The minute excess of entropy, $S_{mag} < 0.1R\ln 2$, associated with

TABLE III. The parameters listed are μ_{Np} and μ_{Co}, the total localized moments on the Np and Co atoms, respectively. $\mu_{L,\,Np}$ and $\mu_{S,\,Np}$ are the orbital and spin contributions to the Np moments. C_2 is the ratio of the orbital and total Np moment. $\mu_{mole} = \mu_{Np} + 2\mu_{Co} + \mu_{int}$ where μ_{int} is the interstitial contribution. The moment values (in μ_B) are reported as a function of the Coulomb U. They are compared to previous LSDA + OP results and experimental data (Ref. 3).

$NpCo_2$	FLL			AMF			OP	Expt.	Expt.*
U (eV)	0.0	1.5	3.0	0.0	1.5	3.0			
μ_{Np}	0.615	1.607	1.986	0.228	1.859	2.596	0.87	0.21(1)	0.63(3)
$\mu_{S,\,Np}$	−1.795	−2.509	−2.727	−2.461	−1.817	−1.295	−2.67	−0.6(1)	−1.8(3)
$\mu_{L,\,Np}$	2.410	4.116	4.713	2.689	3.676	3.891	3.54	0.8(1)	2.4(3)
C_2	3.92	2.56	2.37	11.79	1.98	1.50	4.1	3.7(3)	3.7(3)
μ_{Co}	0.204	0.310	0.314	0.390	0.173	−0.023	0.34	0.06(1)	0.18(3)
μ_{mole}	0.902	2.061	2.473	0.948	2.006	2.512	1.30	0.27(2)	0.81(6)

the magnetic transition indicates that $NpCo_2$ is an itinerant antiferromagnet where the itinerancy of the $5f$ states is due to the strong hybridization between the Co-$3d$ and the Np-$5f$ electrons. The large residual resistivity observed below the metamagnetic transition is related to the antiferromagnetic state of the compound as evidenced by its rapid decrease when the applied field overcomes the metamagnetic field. The linear temperature dependence of the resistivity observed at low temperatures suggests a possible occurrence of a non-Fermi liquid behavior. Electronic structure calculations show that $NpCo_2$ is close to a magnetic instability. Although ferromagnetic arrangement of the Np moments appears to be the ground state, complex AF order cannot be discarded. LSDA + U calculations in the fully localized limit (FLL) where the Coulomb interaction $U \rightarrow 0$ reproduce quite well the total Np moments and their orbital and spin contributions.

ACKNOWLEDGMENTS

We are grateful to B. Lebech, G. H. Lander, and M. Wulff for providing information concerning the characterization of the $NpCo_2$ single crystals. J.P.S. acknowledges F. J. Litterst for fruitful discussions on his muon measurements. The high-purity Np metal required for the fabrication of the $NpCo_2$ compounds was made available through a loan agreement between Lawrence Livermore National Laboratory and ITU, in the framework of a collaboration involving LLNL, Los Alamos National Laboratory, and the U.S. Department of Energy. The support of the European Community—Access to Research Infrastructures action of the Improving Human Potential Programme, European Commission Contract No. RITA-CT-2006-026176 "Actuslab-2," to the Actinide User Laboratory program at ITU-Karlsruhe is acknowledged.

*Present address: Charles University, Faculty of Mathematics and Physics, Department of Condensed Matter Physics, Ke Karlovu 5, CZ-12116 Prague 2, Czech Republic.

†Present address: Institut Jean Lamour, Université de Lorraine, UMR CNRS 7198, Parc de Saurupt, 54042 Nancy cedex, France.

[1] J. Gal, Z. Hadari, U. Atzmony, E. R. Bauminger, I. Nowik, and S. Ofer, Phys. Rev. B **8**, 1901 (1973).

[2] A. T. Aldred, B. D. Dunlap, D. J. Lam, G. H. Lander, M. H. Mueller, and I. Nowik, Phys. Rev. B **11**, 530 (1975).

[3] M. Wulff, O. Eriksson, B. Johansson, B. Lebech, M. S. S. Brooks, G. H. Lander, J. Rebizant, J. C. Spirlet, and P. J. Brown, Europhys. Lett. **11**, 269 (1990).

[4] B. Lebech, M. Wulff, and G. H. Lander, J. Appl. Phys. **69**, 5891 (1991).

[5] O. Eriksson, M. S. S. Brooks, B. Johansson, R. C. Albers, and A. M. Boring, J. Appl. Phys. **69**, 5897 (1991).

[6] J. P. Sanchez, B. Lebech, M. Wulff, G. H. Lander, K. Tomala, K. Mattenberger, O. Vogt, A. Blaise, J. Rebizant, J. C. Spirlet, and P. J. Brown, J. Phys.: Condens. Matter **4**, 9423 (1992).

[7] H. Hill, in *Plutonium 1970 and Other Actinides*, edited by W. N. Miner (AIME, New York, 1971), p. 29.

[8] V. Sechovsky and L. Havela, in *Ferromagnetic Materials*, edited by E. P. Wohlfarth and K. H. J. Buschow (North Holland, Amsterdam, 1988), Vol. 4, p. 309.

[9] G. M. Kalvius, D. R. Noakes, and O. Hartmann, in *Handbook on the Physics and Chemistry of Rare Earths*, edited by K. A. Gschneidner, Jr., L. Eyring, and G. H. Lander (Elsevier Science, Amsterdam, 2001), Vol. 32, p. 55.

[10] G. M. Kalvius, W. Potzel, J. Moser, F. J. Litterst, L. Asch, J. Zänkert, U. Potzel, A. Kratzer, M. Wunsch, J. Gal, S. Fredo, D. Dayan, M. P. Dariel, M. Bogé, J. Chappert, J. C. Spirlet, U. Benedict, and B. D. Dunlap, Physica B **130**, 393 (1985).

[11] M. Wulff (private communication).

[12] J. M. M. Franse, P. H. Frings, F. R. de Boer, and A. Menosvky, in *Physics of Solids under High Pressure*, edited by J. S. Schilling and R. N. Shelton (North Holland, Amsterdam, 1981), p. 181.

[13] R. J. Trainor, M. B. Brodsky, and H. V. Culbert, Phys. Rev. Lett. **34**, 1019 (1975).

[14] P. H. Frings and J. J. M. Franse, Phys. Rev. B **31**, 4355 (1985).

[15] K. Ikeda and K. A. Gschneidner, Jr., Phys. Rev. Lett. **45**, 1341 (1980).

[16] M. T. Béal-Monod, S. K. Ma, and D. R. Fredkin, Phys. Rev. Lett. **20**, 929 (1968).

[17] E. Colineau, P. Javorsky, P. Boulet, F. Wastin, J. C. Griveau, J. Rebizant, J. P. Sanchez, and G. R. Stewart, Phys. Rev. B **69**, 184411 (2004).

[18] J. P. Sanchez, D. Aoki, R. Eloirdi, P. Gaczynski, J. C. Griveau, E. Colineau, and R. Caciuffo, J. Phys.: Condens. Matter **23**, 295601 (2011).

[19] A. Purwanto, R. A. Robinson, L. Havela, V. Sechovsky, P. Svoboda, H. Nakotte, K. Prokes, F. R. de Boer, A. Seret, J. M. Winand, J. Rebizant, and J. C. Spirlet, Phys. Rev. B **50**, 6792 (1994).

[20] E. Brück, H. Nakotte, F. R. de Boer, P. F. de Châtel, H. P. van der Meulen, J. J. M. Franse, A. A. Menovsky, N. H. Kim-Ngan, L. Havela, V. Sechovsky, J. A. A. J. Perenboom, N. C. Tuan, and J. Sebek, Phys. Rev. B **49**, 8852 (1994).

[21] P. Javorský, L. Havela, F. Wastin, P. Boulet, and J. Rebizant, Phys. Rev. B **69**, 054412 (2004).

[22] M. B. Brodsky and R. J. Trainor, Physica B **86-88**, 143 (1977).

[23] G. R. Stewart, B. Andraka, J. S. Kim, and R. G. Haire, Phys. Rev. B **41**, 9336 (1990).

[24] A. B. Shick, A. I. Liechtenstein, and W. E. Pickett, Phys. Rev. B **60**, 10763 (1999).

[25] T. Jeong, A. Kyker, and W. E. Pickett, Phys. Rev. B **73**, 115106 (2006).

[26] A. B. Shick and W. E. Pickett, Phys. Rev. Lett. **86**, 300 (2001).

[27] K. Moore and G. van der Laan, Rev. Mod. Phys. **81**, 235 (2009).